# NONLINEAR DYNAMICS OF AN ORCHARD TOWER SPRAYER BASED ON A DOUBLE INVERTED PENDULUM MODEL

**S. Sartori Junior**
Máquinas Agrícolas Jacto S.A., Rua Dr. Luiz Miranda 1650, Pompéia, 17580-000, SP, Brazil.
sartorijunior@jacto.com.br.br

**J.M. Balthazar**
Department of Statistics, Applied Mathematics and Computation, State University of São Paulo, Rio Claro, PO Box 178, 13500-230, SP, Brazil.
jmbaltha@rc.unesp.br

**B.R. Pontes**
Department of Mechanical Engineering, State University of São Paulo, Bauru, SP, Brazil.
brpontes@feb.unesp.br

***Abstract.*** *In the agriculture field, modern equipments to spray chemicals on orchards consists essentially of a vertical structure, with funs and spray nozzles attached, assembled on a vehicle that travels beside the plants. In a simple construction the vertical structure is attached directly behind the agricultural tractor. In a more complex construction, the vertical structure is attached on a trailer, with or without suspension. In some situations, the lateral oscillations could affect negatively the results of the treatment. Thus, is important to recognize and even control theses lateral oscillations. In this paper, we propose a nonlinear dynamic model for the roll movement analysis of a tower sprayer traveling through orchards. The model is based on the double inverted pendulum model and can be used for simple orchard sprayer assembled directly on trailers, as well as for that ones assembled on trailers, with or without suspension. The models were deduced with Lagrange's equations and Hamilton's principle. The model was implemented on the MatLab® –Simulink® that was used to simulate de roll movements for each type of orchard sprayer in different conditions.*

***Keywords****: nonlinear dynamic model, numerical simulation, tower sprayer, orchard sprayer*

## 1. INTRODUCTION

Traditional orchard spray with one central fan behind the equipment has been replaced by new design machine, with several fans placed on a vertical tower. These kinds of equipment produce air flows convergent and perpendicular to crop surface, they can be better adapted to crop geometry, are more efficient and produce less air and soil contaminations. The height tower, around 6 m, increase the vibrations problems produced by the agricultural irregular soils. Figure 1 shows this kind of orchard sprayer, developed by Máquinas Agrícolas Jacto S/A. It has several fans (1), air nozzles (2) and spray jets (3). The chemicals are storage on the tank (5) and pumped to spray jets by the chemical pump (4). The fans are supported by several structures (6), (7), (8), (9) and (10), which allow adequate positions between the fans and crop plant. The trailer has rigid axles and high flotation agricultural tires.

## 2. OBJECTIVES

This paper objectifies a) to present a mathematical model for the tower orchard sprayers dynamic study; b) to do a transient-response analysis; c) to do a frequency response analysis; d) to find adequate parameters that can aid the project development, before the construction of the equipment.

## 3. MATHEMATIC MODELING

The equipment on Fig.1 is very complex. It has several degrees of freedom. The stability problem in interest is the lateral oscillations of the tower sprayer, called from now roll movement. Figure 2 illustrate a simplified model for this equipment considering only the roll movement. Figure 2a shows the model in the equilibrium position. Figure 2b shows the model out of equilibrium position. The simplified model consists of a trailer with mass $m_1$, with two tires; the tower is represented by a concentrated mass $m_2$ supported by a bar with $L_2$ length and without weight. The tower is connected to trailer chassis on the joint P, placed the distance $L_1$ above the gravity center of the trailer. The joint P allows only lateral movements.

Considering an inertial system X-Y this simplified model has tree degrees of freedom: vertical displacement of the trailer gravity centre ($y_1$), trailer angular displacement ($\phi_1$) and tower angular displacement ($\phi_2$). The lateral displacement of the trailer gravity centre, $x_1$, is limit by tires, is too small comparing to the magnitudes of other displacements. So it is assumed $x_1$ constant.

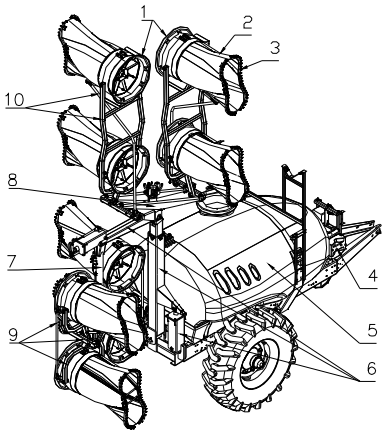


Figure 1: Tower orchard sprayer (Máquinas Agrícolas Jacto S/A courtesy)

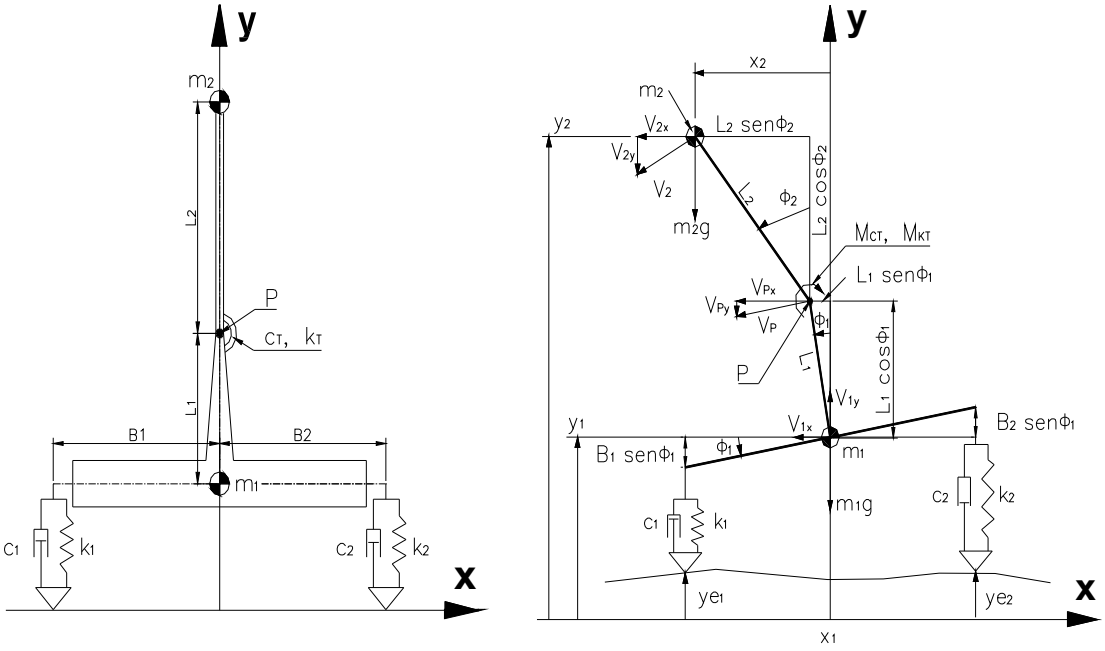


a) b)

Figure 2: Simplified model of the tower sprayer - a) in the equilibrium position - b) out of equilibrium position.

Table 1: Model nomenclature

| | | |
|---|---|---|
| $B_1$: distance from center line of axel trailer to the left tire | $m_1$: trailer mass (concentrate at the gravity centre) | $\dot{x}_2$ : tower horizontal velocity |
| $B_2$: distance from center line of axel trailer to the right tire | $m_2$: tower mass (concentrate at the gravity centre) | $\ddot{x}_2$ : tower horizontal acceleration |
| $C_1$: left tire damping, | $\phi_1$ : trailer angular displacement | $y_1$ : trailer vertical displacement |
| $C_2$: right tire damping | $\dot{\phi}_1$ : trailer angular velocity | $\dot{y}_1$ : trailer vertical velocity |
| $C_T$: joint torsional damping | $\ddot{\phi}_1$ : trailer angular acceleration | $\ddot{y}_1$ : trailer vertical acceleration |
| $I_1$: trailer inertia moment without tower | $\phi_2$ : tower angular displacement | $y_2$ : tower vertical displacement |
| $I_2$: tower inertia moment | $\dot{\phi}_2$ : tower angular velocity | $\dot{y}_2$ : tower vertical velocity |
| $K_1$: left tire stiffness, | $\ddot{\phi}_2$ : tower angular acceleration | $\ddot{y}_2$ : tower vertical acceleration |
| $K_2$: right tire stiffness, | $x_1$ : trailer horizontal displacement | $y_{e1}$ : left tire vertical displacement |
| $K_T$: joint torsional stiffness | $\dot{x}_1$ : trailer horizontal velocity | $\dot{y}_{e1}$ : left tire vertical velocity |
| $L_1$ : distance from the trailer GC to joint P | $\ddot{x}_1$ : trailer horizontal acceleration | $y_{e2}$ : right tire vertical displacement |
| $L_2$ : distance from the tower GC to joint P | $x_2$ : tower horizontal displacement | $\dot{y}_{e2}$ : right tire vertical velocity |

To derive the model equations of movements, one of possible ways is to use Lagrange equations:

$$L = E_C - W_C - W_{NC} \tag{1}$$

And Hamilton principle:

$$\frac{d}{dt}\left(\frac{\partial L}{\partial \dot{q}}\right) - \left(\frac{\partial L}{\partial q}\right) + \left(\frac{\partial F}{\partial \dot{q}}\right) = 0 \tag{2}$$

Where $E_C$ is the kinetic energy, $W_C$ is the work of conservative forces, in this case the potential energy of weight and stiffness forces. $W_{NC}$ is the work of non conservative forces, or energy dissipated from damping forces.

The total kinetic energy form this system is the sum of trailer kinetic energy, $E_{C1}$ , and tower kinetic energy, $E_{C2}$:

$$E_C = E_{C1} + E_{C2} \tag{3}$$

$$E_{C1} = \frac{1}{2} m_1 V_1^{\,2} + \frac{1}{2} I_1 \dot{\phi}_1^{\,2} = \frac{1}{2} m_1 (V_{1x}^{\,2} + V_{1y}^{\,2}) + \frac{1}{2} I_1 \dot{\phi}_1^{\,2} = \frac{1}{2} m_1 (\dot{x}_1^{\,2} + \dot{y}_1^{\,2}) + \frac{1}{2} I_1 \dot{\phi}_1^{\,2} \tag{4}$$

$$E_{C2} = \frac{1}{2} m_2 V_2^{\,2} + \frac{1}{2} I_2 \dot{\phi}_2^{\,2} = \frac{1}{2} m_2 (V_{2x}^{\,2} + V_{2y}^{\,2}) + \frac{1}{2} I_2 \dot{\phi}_2^{\,2} = \frac{1}{2} m_2 (\dot{x}_2^{\,2} + \dot{y}_2^{\,2}) + \frac{1}{2} I_2 \dot{\phi}_2^{\,2} \tag{5}$$

From the geometry of Fig. 3:

$$x_2 = x_1 - L_1 \, sen\phi_1 - L_2 \, sen\phi_2 \tag{6}$$

$$y_2 = y_1 + L_1 \cos\phi_1 + L_2 \cos\phi_2 \tag{7}$$

And their time derivatives:

$$\dot{x}_2 = \dot{x}_1 - L_1 \, \dot{\phi}_1 \cos\phi_1 - L_2 \, \dot{\phi}_2 \cos\phi_2 \tag{8}$$

$$\dot{y}_2 = \dot{y}_1 - L_1 \dot{\phi}_1 \, sen\phi_1 - L_2 \dot{\phi}_2 \, sen\phi_2 \tag{9}$$

The lateral displacements of the trailer gravity center, $x_1$, are too small comparing to the magnitudes of other displacements. So it is assumed that:

$$x_1 \cong cte \Rightarrow \dot{x}_1 = \ddot{x}_1 = 0 \tag{10}$$

Replacing the Eq.(6), Eq.(7), Eq.(8), Eq.(9) and Eq.(10) into Eq.(3), Eq.(4) and Eq.(5):

$$\begin{aligned} E_C = {} & \frac{1}{2}(m_1 + m_2)\dot{y}_1^{\,2} + \frac{1}{2} m_2 L_1^{\,2} \dot{\phi}_1^{\,2} + \frac{1}{2} m_2 L_2^{\,2} \dot{\phi}_2^{\,2} + m_2 L_1 L_2 \dot{\phi}_1 \dot{\phi}_2 \cos(\phi_2 - \phi_1) - m_2 \dot{y}_1 \dot{\phi}_1 L_1 \, sen\phi_1 + \\ & - m_2 \dot{y}_1 \dot{\phi}_2 L_2 \, sen\phi_2 + \frac{1}{2} I_1 \dot{\phi}_1^{\,2} + \frac{1}{2} I_2 \dot{\phi}_2^{\,2} \end{aligned} \tag{11}$$

The total potential energy of this system, $E_P$, is the sum of the trailer potential energy $E_{C1}$ and the tower potential energy $E_{C2}$:

$$E_P = E_{Pm_1} + E_{Pm_2} + E_{PK_1} + E_{PK_2} + E_{PK_T}$$

$$E_P = m_1 \, g \, y_1 + m_2 \, g \, y_2 + \frac{1}{2} K_1 (\Delta y_{K1})^2 + \frac{1}{2} K_2 (\Delta y_{K2})^2 + \frac{1}{2} K_T (\Delta \phi_{K_T})^2$$

$$E_P = m_1 g y_1 + m_2 g y_2 + \frac{1}{2} K_1 (y_1 - B_1 \, sen\phi_1 - y_{e_1})^2 + \frac{1}{2} K_2 (y_1 + B_2 \, sen\phi_1 - y_{e_2})^2 + \frac{1}{2} K_T (\phi_2 - \phi_1)^2 \tag{12}$$

Where $E_{Pm_1}, E_{Pm_2}, E_{PK_1}, E_{PK_2}, E_{PK_T}$ are respectively the potentials energies of the trailer, the tower, the left tire, the right tire and the joint torsional. $\Delta y_{K_1}, \Delta y_{K_2}, \Delta y_{K_T}$ are respectively the deformations of the left tire, the right tire and the torsional joint. Replacing Eq.(7) into Eq.(12) and developing it, results:

$$\begin{aligned} E_P = {} & (m_1 + m_2) g \, y_1 + m_2 \, g \, L_1 \cos\phi_1 + m_2 \, g \, L_2 \cos\phi_2 + \frac{1}{2} K_1 \, y_1^{\,2} + \frac{1}{2} K_1 \, B_1^{\,2} \, sen^2\phi_1 + \frac{1}{2} K_1 \, y_{e_1}^{\,2} - \\ & K_1 \, y_1 \, B_1 \, sen\phi_1 - K_1 \, y_1 \, y_{e_1} + K_1 \, y_{e_1} \, B_1 \, sen\phi_1 + \frac{1}{2} K_2 \, y_1^{\,2} + \frac{1}{2} K_2 \, B_2^{\,2} \, sen^2\phi_1 + \frac{1}{2} K_2 \, y_{e_2}^{\,2} + \\ & K_2 \, y_1 \, B_2 \, sen\phi_1 - K_2 \, y_1 \, y_{e_2} - K_2 \, y_{e_2} \, B_2 \, sen\phi_1 + \frac{1}{2} K_T \, \phi_2^{\,2} + \frac{1}{2} K_T \, \phi_1^{\,2} - K_T \, \phi_1 \, \phi_2 \end{aligned} \tag{13}$$

The total system damping F is the sum of the dissipation energy on tires and torsional joint, respectively $F_{C_1}, F_{C_2}$ and $F_{C_T}$ :

$$F = F_{C_1} + F_{C_2} + F_{C_T}$$

$$F = \frac{1}{2} C_1 (\Delta \dot{y}_{C1})^2 + \frac{1}{2} C_2 (\Delta \dot{y}_{C2})^2 + \frac{1}{2} C_T (\Delta \dot{\phi}_{CT})^2 \tag{14}$$

Where $\Delta\dot{y}_{C1}, \Delta\dot{y}_{C2}, \Delta\dot{y}_{CT}$ are respectively the time rate deformations of the left tire, the right tire and the torsional joint, deduced from figure 2b.

$$F = \frac{1}{2}C_1\left(\dot{y}_1 - B_1\dot{\phi}_1\cos\phi_1 - \dot{y}_{e_1}\right)^2 + \frac{1}{2}C_2\left(\dot{y}_1 + B_2\dot{\phi}_1\cos\phi_1 - \dot{y}_{e_2}\right)^2 + \frac{1}{2}C_T\left(\dot{\phi}_2 - \dot{\phi}_1\right)^2 \tag{15}$$

$$F = \frac{1}{2}(C_1+C_2)\dot{y}_1^{\,2} + \frac{1}{2}\left(C_1B_1^{\,2} + C_2B_2^{\,2}\right)\dot{\phi}_1^{\,2}\cos^2\phi_1 + (C_2B_2 - C_1B_1)\dot{y}_1\dot{\phi}_1\cos\phi_1 + \frac{1}{2}C_1\dot{y}_{e1}^{\,2} + \frac{1}{2}C_2\dot{y}_{e2}^{\,2} - C_1\dot{y}_1\dot{y}_{e1} - C_2\dot{y}_1\dot{y}_{e2} + C_1B_1\dot{y}_{e1}\dot{\phi}_1\cos\phi_1 - C_2B_2\dot{y}_{e2}\dot{\phi}_1\cos\phi_1 + \frac{1}{2}C_T\dot{\phi}_2^{\,2} - C_T\dot{\phi}_1\dot{\phi}_2 + \frac{1}{2}C_T\dot{\phi}_1^{\,2} \tag{16}$$

Using de Hamilton principle for $y_1$ results:

$$\frac{d}{dt}\left(\frac{\partial L}{\partial\dot{y}_1}\right) - \left(\frac{\partial L}{\partial y_1}\right) + \left(\frac{\partial F}{\partial\dot{y}_1}\right) = 0 \tag{17}$$

$$(m_1+m_2)\ddot{y}_1 - m_2L_1\ddot{\phi}_1\,sen\phi_1 - m_2L_2\ddot{\phi}_2\,sen\phi_2 - m_2L_1\dot{\phi}_1^{\,2}\cos\phi_1 - m_2L_2\dot{\phi}_2^{\,2}\cos\phi_2 + (C_1+C_2)\dot{y}_1 + (C_2B_2 - C_1B_1)\dot{\phi}_1\cos\phi_1 + (K_1+K_2)y_1 + (K_2B_2 - K_1B_1)sen\phi_1 + (m_1+m_2)g = K_1y_{e1} + K_2y_{e2} + C_1\dot{y}_{e1} + C_2\dot{y}_{e2} \tag{18}$$

Using de Hamilton principle for $\phi_1$ results:

$$\frac{d}{dt}\left(\frac{\partial L}{\partial\dot{\phi}_1}\right) - \left(\frac{\partial L}{\partial\phi_1}\right) + \left(\frac{\partial F}{\partial\dot{\phi}_1}\right) = 0 \tag{19}$$

$$-m_2L_1sen\phi_1\ddot{y}_1 + (I_1+m_2L_1^2)\ddot{\phi}_1 + m_2L_1L_2\cos(\phi_2-\phi_1)\ddot{\phi}_2 - m_2L_1L_2sen(\phi_2-\phi_1)\dot{\phi}_2^2 + (C_2B_2 - C_1B_1)\cos\phi_1\dot{y}_1 + (C_T + (C_1B_1^2 + C_2B_2^2)\cos^2\phi_1)\dot{\phi}_1 - C_T\dot{\phi}_2 + (K_2B_2 - K_1B_1)\cos\phi_1\,y_1 + K_T\phi_2 + (K_1B_1^2 + K_2B_2^2)sen\phi_1\cos\phi_1 - m_2gL_1sen\phi_1 = -K_1B_1\cos\phi_1\,y_{e1} + K_2B_2\cos\phi_1\,y_{e2} - C_1B_1\cos\phi_1\,\dot{y}_{e1} + C_2B_2\cos\phi_1\,\dot{y}_{e2} \tag{20}$$

Finally, using de Hamilton principle for $\phi_2$ results:

$$\frac{d}{dt}\left(\frac{\partial L}{\partial\dot{\phi}_2}\right) - \left(\frac{\partial L}{\partial\phi_2}\right) + \left(\frac{\partial F}{\partial\dot{\phi}_2}\right) = 0 \tag{21}$$

$$-m_2L_2sen\phi_2\ddot{y}_1 + m_2L_1L_2\cos(\phi_2-\phi_1)\ddot{\phi}_1 + (I_2+m_2L_2^2)\ddot{\phi}_2 + m_2L_1L_2sen(\phi_2-\phi_1)\dot{\phi}_1^2 + -C_T\dot{\phi}_1 + C_T\dot{\phi}_2 - K_T\phi_1 + K_T\phi_2 - m_2gL_2sen\phi_2 = 0 \tag{22}$$

Equations (18), (20) and (22) represent the motion equations of the non linear model shown on Fig.3, which rearranged in the matrix form, results:

$$\begin{bmatrix} m_1+m_2 & -m_2L_1sen\phi_1 & -m_2L_2sen\phi_2 \\ -m_2L_1sen\phi & I_1+m_2L_1^{\,2} & m_2L_1L_2\cos(\phi_2-\phi_1) \\ -m_2L_2sen\phi_2 & m_2L_1L_2\cos(\phi_2-\phi_1) & I_2+m_2L_2^{\,2} \end{bmatrix}\begin{bmatrix}\ddot{y}_1\\ \ddot{\phi}_1\\ \ddot{\phi}_2\end{bmatrix} + \begin{bmatrix} 0 & -m_2L_1\cos\phi_1 & -m_2L_2\cos\phi_2 \\ 0 & 0 & -m_2L_1L_2sen(\phi_2-\phi_1) \\ 0 & -m_2L_1L_2sen(\phi_2-\phi_1) & 0 \end{bmatrix}\begin{bmatrix}\dot{y}_1^{\,2}\\ \dot{\phi}_1^{\,2}\\ \dot{\phi}_2^{\,2}\end{bmatrix} + \begin{bmatrix} C_1+C_2 & (C_2B_2-C_1B_1)\cos\phi_1 & 0 \\ (C_2B_2-C_1B_1)\cos\phi_1 & C_T+(C_1B_1^{\,2}+C_2B_2^{\,2})\cos^2\phi_1 & -C_T \\ 0 & -C_T & C_T \end{bmatrix}\begin{bmatrix}\dot{y}_1\\ \dot{\phi}_1\\ \dot{\phi}_2\end{bmatrix} + \begin{bmatrix} K_1+K_2 & 0 & 0 \\ (K_2B_2-K_1B_1)\cos\phi_1 & K_T & -K_T \\ 0 & -K_T & K_T \end{bmatrix}\begin{bmatrix}y_1\\ \phi_1\\ \phi_2\end{bmatrix} + \begin{bmatrix}(K_2B_2-K_1B_1)sen\phi_1 + (m_1+m_2)g \\ (K_1B_1^{\,2}+K_2B_2^{\,2})sen\phi_1\cos\phi_1 - m_2gL_1sen\phi_1 \\ -m_2gL_2sen\phi_2\end{bmatrix} = \begin{bmatrix} K_1y_{e1} + K_2y_{e2} + C_1\dot{y}_{e1} + C_2\dot{y}_{e2} \\ -K_1B_1\cos\phi_1\,y_{e1} + K_2B_2\cos\phi_1\,y_{e2} - C_1B_1\cos\phi_1\,\dot{y}_{e1} + C_2B_2\cos\phi_1\,\dot{y}_{e2} \\ 0\end{bmatrix} \tag{23}$$

In case of small angular displacements, it can be assumed $sen\phi \cong \phi$, $\cos\phi \cong 1$ and $\phi\ddot{y} \cong \phi\ddot{\phi} \cong \dot{y}^2 \cong 0$, resulting on the motion equations of the linear model:

$$\begin{bmatrix} m_1+m_2 & 0 & 0 \\ 0 & I_1+m_2L_1^2 & m_2L_1L_2 \\ 0 & m_2L_1L_2 & I_2+m_2L_2^2 \end{bmatrix}\begin{bmatrix} \ddot{y}_1 \\ \ddot{\phi}_1 \\ \ddot{\phi}_2 \end{bmatrix}+\begin{bmatrix} C_1+C_2 & C_2B_2-C_1B_1 & 0 \\ C_2B_2-C_1B_1 & C_T+C_1B_1^2+C_2B_2^2 & -C_T \\ 0 & -C_T & C_T \end{bmatrix}\begin{bmatrix} \dot{y}_1 \\ \dot{\phi}_1 \\ \dot{\phi}_2 \end{bmatrix}+$$
$$+\begin{bmatrix} K_1+K_2 & K_2B_2-K_1B_1 & 0 \\ K_2B_2-K_1B_1 & K_T+K_1B_1^2+K_2B_2^2-m_2gL_1 & -K_T \\ 0 & -K_T & K_T-m_2gL_2 \end{bmatrix}\begin{bmatrix} y_1 \\ \phi_1 \\ \phi_2 \end{bmatrix}+\begin{bmatrix} (m_1+m_2)g \\ 0 \\ 0 \end{bmatrix}=\begin{bmatrix} K_1y_{e1}+K_2y_{e2}+C_1\dot{y}_{e1}+C_2\dot{y}_{e2} \\ -K_1B_1y_{e1}+K_2B_2y_{e2}-C_1B_1\dot{y}_{e1}+C_2B_2\dot{y}_{e2} \\ 0 \end{bmatrix} \quad (24)$$

Theses motion equations, non linear Eq.(23) and linear models Eq.(24), were implemented on Matlab© Simulink© to find $y_1, \dot{y}_1, \phi_1, \dot{\phi}_1, \phi_2$ *e* $\dot{\phi}_2$ , and finally, to calculate the tower displacements $x_2$ e $y_2$ using Eq.(6) and Eq.(7).

## 4. DYNAMIC ANALYSIS

### 4.1. The models parameters

The values for tires stiffness and damping were supplied by the Máquinas Agrícolas Jacto S/A laboratory. The trailer and tower masses, trailer and tower inertial moment were deduced from the sprayer project. The trailer mass consider the tank full of water. The lengths $B_1$, $B_2$, $L_1$ and $L_2$, also deduced from the sprayer project, were assumed constants. This way, $K_T$ and $C_T$ are the simulation variables to analyze the dynamic of models in different exciting conditions.

Table 2: Model parameters

| | | | | |
|---|---|---|---|---|
| $B_1 = B_2 = 0{,}8$ m | $K_1 = 467000$ N/m | $I_1 = 6850$ kg m$^2$ | $L_1 = 0{,}2$ m | $m_1 = 6500$ kg |
| $C_1 = C_2 = 2500$ Ns/m | $K_2 = 467000$ N/m | $I_2 = 6250$ kg m$^2$ | $L_2 = 2{,}4$ m. | $m_2 = 800$ kg |

### 4.2. Transient Analysis - Torsional Stiffness ($K_T$) selection

First, both models, linear and non linear, were simulate using the input of a step signal on the left tire ( $y_{e1}$ ): amplitude of 0,2 meter in time 0,8 seconds. The right tire was not excited ( $y_{e2} = 0$ ). The joint torsional stiffness was set in a wide range of values (100 Nm/rad < $K_T$ < 1000000 Nm/rad). The joint torsional damping was set at constant in a low value ($C_T$ =1000 Nms/rad). Figure 3 show some of the results of lateral displacements of the tower $x_2$ according to the non linear model (x2 NL; continuous line) and according to the linear model (x2 L; dashed line). Figure 4 shows the angular displacement of the trailer (phi1=$\phi_1$) and tower (phi2=$\phi_2$) for the non linear model. Figure 5 shows the angular displacement of the trailer (phi1=$\phi_1$) and tower (phi2=$\phi_2$) for the linear model.

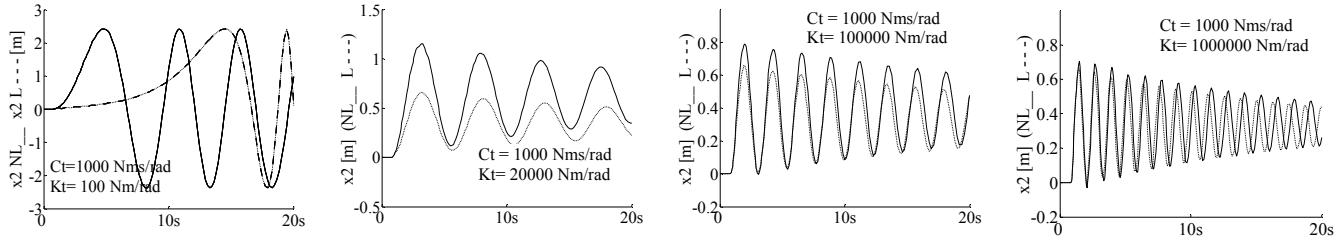


a) b) c) d)

Figure 3: Lateral displacement of the tower ($x_2$) according to non linear model (continuous line) and linear model (dashed line).

For small values of $K_T$ , both models indicate big lateral displacements of the tower. The result of the linear model notable differs of the non linear model. In this situation the linear model can't be used, once it is false the condition of small angles assumed for its linearization ( $sen\phi \neq \phi$, $\cos\phi \neq 1$ and $\phi\ddot{y} \neq \phi\ddot{\phi} \neq \dot{y}^2 \neq 0$ ). The results from the non linear model are more trustful, once there are no considerations about angles size. Note that increasing the $K_T$ the results of the linear and non linear models become closer. For a very low value of $K_T$ (Kt=100 Nm/rad), the tower it inclines totally (see NL phi2 - figure 4a). For a Kt = 20000 Nm/rad the tower oscillate laterally. The oscillation period of the

linear model result become similar of the non linear one, but its amplitude is notable smaller. For big values of $K_T$ ($K_T$ > 100.000 Nm/rad) the results of the linear and the non linear models become similar.

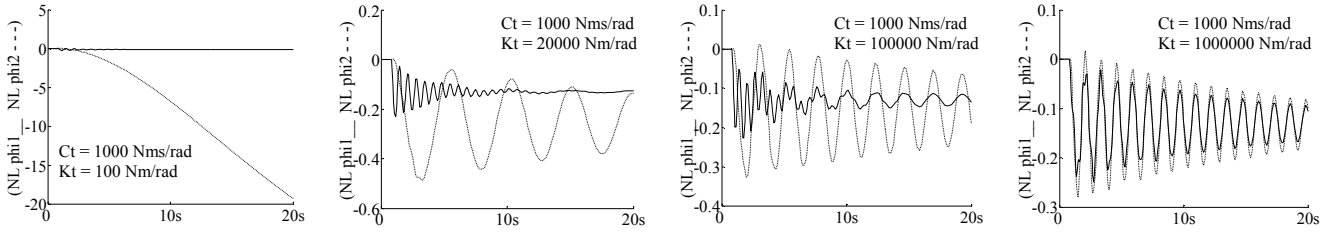


Figure 4: Angular displacement of the trailer (NL phi 1, continuous line) and tower (NL phi 2, dashed line) with a step input on the left tire, according to the non linear model.

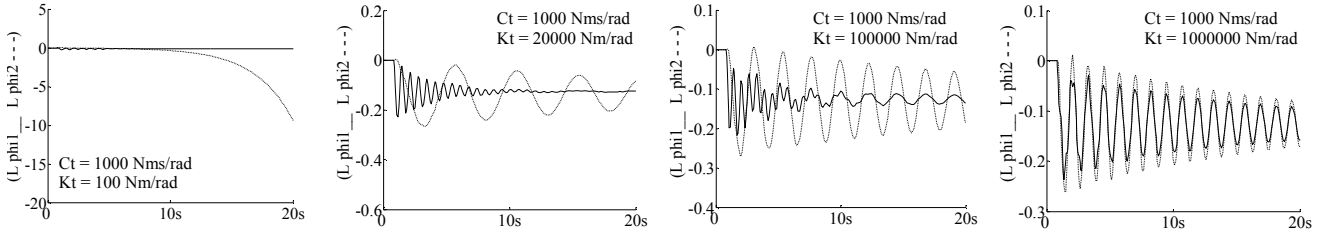


Figure 5: Angular displacement of the trailer (L phi 1, continuous line) and of the tower (L phi 2, dashed line), with a step input on the left tire, according to the linear model.

With small values of $K_T$, a flexible trailer-tower joint, the natural frequency of tower is too little than the trailer ones (see figure 4b and figure5b). With a flexible trailer-tower joint, the tower oscillates with slow frequency and big angles than with a rigid joint trailer-tower (compare figures 3b with 3c, figures 4b with 4c and figures 5b with 5c). With a flexible trailer-tower joint the natural frequencies of the tower and the trailer are distinctive, and there is little interference from the tower oscillation into the trailer oscillation. There is no coupling between trailer and tower. With a hard joint trailer-tower (figures 3d, 4d and 5d) there is big coupling between trailer and tower. Tower and trailer oscillate as a unique body over the tires.

### 4.3. Transient Analysis - Torsional Damping ($C_T$) selection

During the previous analysis was assumed a low value for torsional damping, $C_T$. For a sensibility torsional damping, $C_T$ analysis, both models were submitted a step input of 0,2m at 0,8s on the left tire, $y_{e1}$. The $K_T$ parameter was set constant at 100000 Nm/rad. Figure 6 compares the lateral displacement of the tower, $x_2$, for both model $C_T$ changing in the range of 10000 until 200000 Nms/rad.

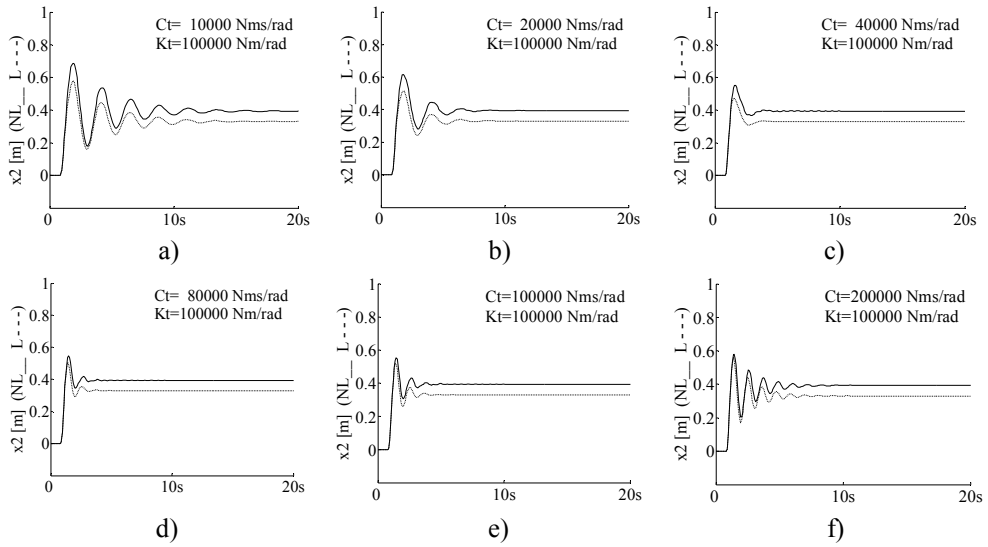


Figure 6: Lateral displacement of tower, $x_2$, for the non linear model (continuous line) and for the linear model (dashed line), using a step input of 0,2m at 0,8s on the left tire, $y_{e1}$, changing $C_T$ between 10000 until 200000 Nms/rad, with $K_T$ fixed at 100000 Nm/rad.

Figure 7 compares the angular displacement of the trailer (phi1=$\phi_1$; continuous line) and tower (phi2=$\phi_2$; dashed line) for the non linear model, using a step input of 0,2m at 0,8s on the left tire, $y_{e1}$, changing $C_T$ between 10000 until 200000 Nms/rad, with $K_T$ fixed at 100000 Nm/rad.

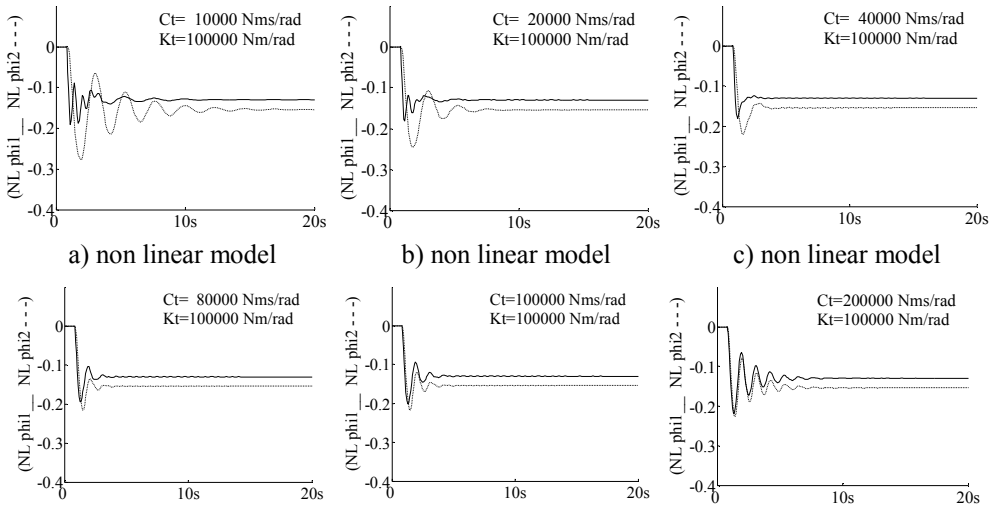


a) non linear model b) non linear model c) non linear model

d) non linear model e) non linear model f) non linear model

Figure 7: Angular displacement of trailer (phi1=$\phi_1$; continuous line) and tower (phi2=$\phi_2$; dashed line) for the non linear model, using a step input of 0,2m at 0,8s on the left tire, $y_{e1}$, changing $C_T$ between 10000 until 200000 Nms/rad. $K_T$ set at 100000 Nm/rad.

Figure 8 compares the angular displacement of the trailer (phi1=$\phi_1$; continuous line) and tower (phi2=$\phi_2$; dashed line) for the linear model, using a step input of 0,2m at 0,8s on the left tire, $y_{e1}$, changing $C_T$ between 10000 until 200000 Nms/rad, with $K_T$ fixed at 100000 Nm/rad.

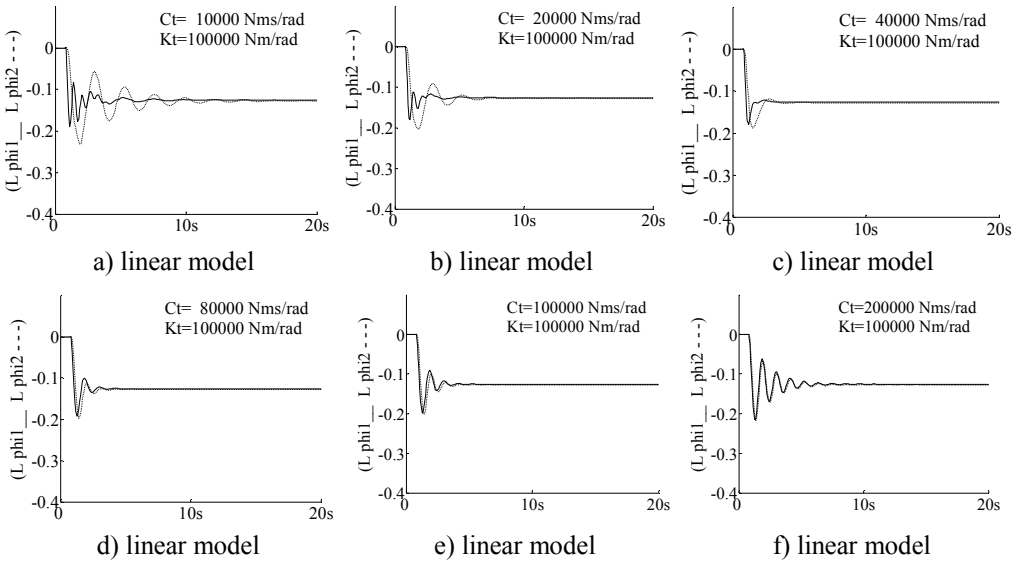


a) linear model b) linear model c) linear model

d) linear model e) linear model f) linear model

Figure 8: Angular displacement of trailer (phi1=$\phi_1$; continuous line) and tower (phi2=$\phi_2$; dashed line) for the linear model, using a step input of 0,2m at 0,8s on the left tire, $y_{e1}$, changing $C_T$ between 10000 until 200000 Nms/rad. $K_T$ set at 100000 Nm/rad.

$K_T$ was set at 100000 Nm/rad because this value produces small angular displacements of tower. Thus the linearization of linear model is valid and the answers of both modes can be compared.

As show in figures 6, 7 and 8 increasing $C_T$ from 10000 Nms/rad to 40000 Nms/rad was possible to reduce the tower oscillation setting time. But, continuing to increasing de torsional damping until 200000 Nms/rad the setting time increases. These effects can be explained by the coupling between tower and trailer: low values of $C_T$ produce few

coupling between tower and trailer; high values of $C_T$ produce a big coupling between tower and trailer. Similar as shown in the $K_T$ analysis, with low values of $C_T$ tower and trailer oscillate with distinctive natural frequencies, with high $C_T$ values tower and trailer oscillate as a unique body over the tires. These results, confirm that is possible to find optimum values for stiffness and damping with both models.

When the orchard sprayer, traveling on agricultural field, cross over an obstacle the tower incline left or right, but it is desirable it returns quickly to equilibrium position. The careful analysis of the system answer with a step input can indicates how good the selection of $K_T$ and $C_T$ parameters were.

According Ogata (1982) "for a desirable transient response, quickly and sufficiently damped, a second order of a second-order system, the damping ratio ($\zeta$) must be between 0,4 and 0,8. Small values of $\zeta$ ($\zeta$<0,4) yield excessive overshoot in the transient response, and a system with a large value of $\zeta$ ($\zeta$>0,8) responds sluggishly." Where the damping ratio ($\zeta$) is:

$$\zeta = \frac{C_T}{2\sqrt{K_T\ I_2}} \tag{23}$$

Note that for $K_T$ of 100000 Nm/rad and $C_T$ of 40000 Nms/rad the damping ratio $\zeta$ is 0,8 the maximum overshoot ($M_p$) is 37,5%, the settling time ($t_s$) is 1,4 seconds for an allowable tolerance of 10% and the tower oscillates for one cycle (see figure 9). In this study a maximum overshoot of 15 cm and a settling time of 1,4 second are reasonable.

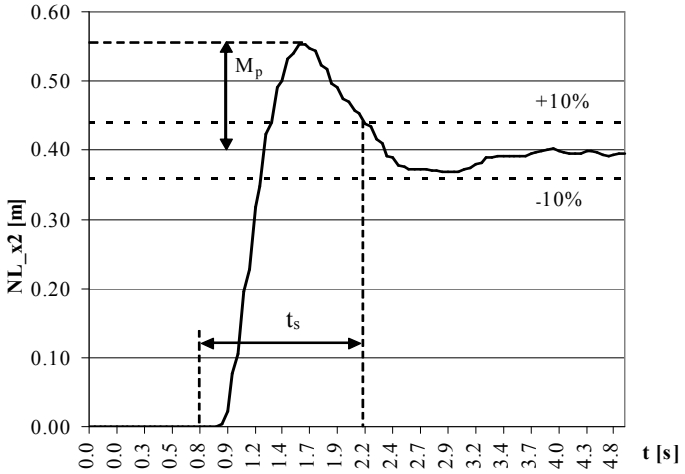


Figure 9: Lateral displacement of tower, $x_2$, for the non linear model, with a step input of 0,2m at 0,8s on the left tire, $y_{e1}$; $K_T$ = 100000 Nm/rad; $C_T$ = 40000 Nms/rad.

### 4.4. Frequency Response Analysis

For the frequency response analysis the non linear model was exited by a sinusoidal wave at the left tire, $y_{e1}$= 0,1 sin (wt), The frequency (w) set between 1 up to 20 rad/s. There was no input at the right tire ($y_{e1}$=0). $K_T$ was fixed at 100000 Nm/rad and $C_T$ was set between 5000 up to 40000 Nms/rad.

Figure 10 shows the magnitude ratio (tower lateral displacement amplitude $x_2$ peak-to-peak divided by sinusoidal amplitude peak-to-peak) versus sinusoidal input frequency. The tower natural frequency is around 3 rad/s, wile the trailer natural frequency is around 11 rad/s.

When the orchard sprayer travel over an irregular soil surface the input signal on tires consist of a large range of frequencies (w). As show in figure 10 if the input frequency is near the tower natural frequency, the suspension on joint P can not isolate the system. There are big lateral amplitudes of the tower. The tower response amplitude is inversely proportional of $C_T$ value. With a low $C_T$ ($C_T$=5000 Nms/rad) the lateral amplitudes of tower are bigger than with higher $C_T$ ($C_T$=40000 Nms/rad). Otherwise if the input frequencies are over the natural frequency of tower (w > 5 rad/s) the movement of the tower can be isolate from trailer. In these cases, there is few influence of $C_T$ value.

### 4.5. Field Response Analysis

The sprayer response analysis with a step input and a sinusoidal input are very useful in the project definition, but is important have in mind that these simples inputs rarely represents the real conditions found in agricultural field.

To analyze the field response of this system, the ISO-5008 (1979) artificial smoother track was used as input signal on the left tire ($y_{e1}$) and the right tire ($y_{e2}$) simultaneously. This track consists basically by several obstacles with different heights, each other separated by 160mm, along 100m length. Figure 11 represents the surface of this track for the left tire (continuous line) and for the right tire (dashed line).

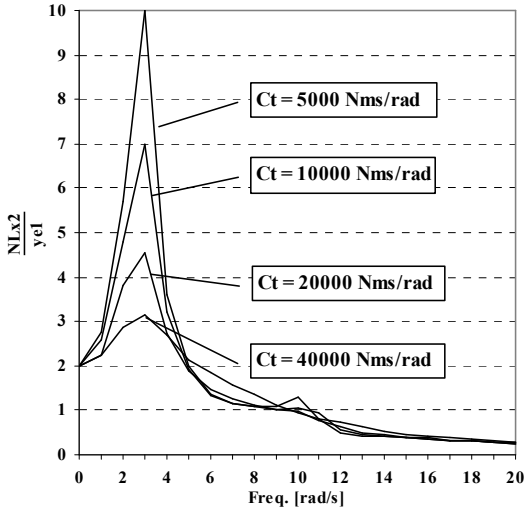


Figure 10: Amplitude Response Peak-to-Peak between tower lateral displacement (NL_x2) and input amplitude (ye1) for the non linear model, $K_T$ =100000 Nm/rad e $C_T$ from 5000 Nms/rad until 40000 Nms/rad.

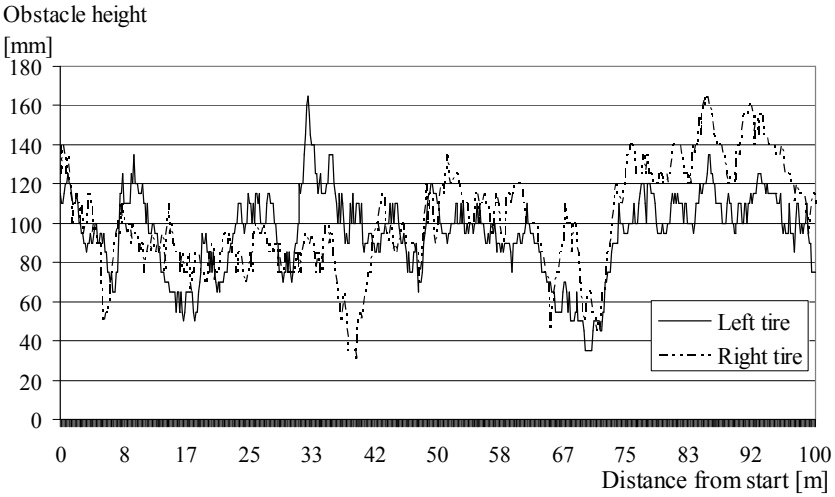


Figure 11: Surface of the ISO5008 (1979) artificial smoother track.

Table 3 compares the tower responses, lateral displacements ( $x_2$ ) and acceleration ( $\ddot{x}_2$ ) using non linear model and the ISO5008 (1979) artificial smoother track signal input with three travel speeds of the sprayer. Table 4 compares the same for the linear model.

Table 3: Responses of the tower lateral displacement and acceleration with a soft joint versus a hard joint, with the non linear model, using the ISO5008 (1979) artificial smoother track signal input.

| **Non linear model** | Lateral Displacement $x_2$ [m] | | | Lateral Acceleration $\ddot{x}_2$ [m/s$^2$] | | |
|---|---|---|---|---|---|---|
| | Soft Joint $K_T$ = 100000 Nm/rad $C_T$ = 40000 Nms/rad | Hard Joint $K_T$ =5000000 Nm/rad $C_T$ = 40000 Nms/rad | Ratio Hard / Soft | Soft Joint $K_T$ =100000 Nm/rad $C_T$ =40000 Nms/rad | Hard Joint $K_T$ =5000000 Nm/rad $C_T$ = 40000 Nms/rad | Ratio Hard / Soft |
| Speed 3 km/h | 0,273 (max-min) | 0,273 (max-min) | 1,0 | 1,70 (max-min) | 1,70 (max-min) | 1,0 |
| Speed 6 km/h | 0,264 (max-min) | 0,504 (max-min) | 1,9 | 2,74 (max-min) | 14,27 (max-min) | 5,2 |
| Speed 12 km/h | 0,256 (max-min) | 0,574 (max-min) | 2,2 | 3,77 (max-min) | 16,54 (max-min) | 4,4 |
| Speed 3 km/h | 0,052 (average) | 0,052 (average) | 1,0 | 0,29 (average) | 0,29 (average) | 1,0 |
| Speed 6 km/h | 0,053 (average) | 0,101 (average) | 1,9 | 0,44 (average) | 2,75 (average) | 6,3 |
| Speed 12 km/h | 0,053 (average) | 0,114 (average) | 2,2 | 0,62 (average) | 3,23 (average) | 5,2 |

Table 4: Responses of the tower lateral displacement and acceleration with a soft joint versus a hard joint. Linear model with the ISO5008 (1979) artificial smoother track signal input.

| **Linear model** | Lateral Displacement $x_2$ [m] | | | Lateral Acceleration $\ddot{x}_2$ [m/s$^2$] | | |
|---|---|---|---|---|---|---|
| | Soft Joint $K_T$ = 100000 Nm/rad $C_T$ = 40000 Nms/rad | Hard Joint $K_T$ = 5000000 Nm/rad $C_T$ = 40000 Nms/rad | Ratio Hard / Soft | Soft Joint $K_T$ = 100000 Nm/rad $C_T$ = 40000 Nms/rad | Hard Joint $K_T$ = 5000000 Nm/rad $C_T$ = 40000 Nms/rad | Ratio Hard / Soft |
| Speed 3 km/h | 0,235 (max-min) | 0,235 (max-min) | 1,0 | 1,69 (max-min) | 1,69 (max-min) | 1,0 |
| Speed 6 km/h | 0,230 (max-min) | 0,467 (max-min) | 2,0 | 2,60 (max-min) | 12,30 (max-min) | 4,7 |
| Speed 12 km/h | 0,226 (max-min) | 0,530 (max-min) | 2,4 | 3,78 (max-min) | 13,88 (max-min) | 3,7 |
| Speed 3 km/h | 0,045 (average) | 0,045 (average) | 1,0 | 0,28 (average) | 0,28 (average) | 1,0 |
| Speed 6 km/h | 0,046 (average) | 0,088 (average) | 1,9 | 0,43 (average) | 2,42 (average) | 5,6 |
| Speed 12 km/h | 0,046 (average) | 0,119 (average) | 2,6 | 0,60 (average) | 3,47 (average) | 5,8 |

In tables 3 and 4 are present two groups of responses: the tower lateral displacements and the tower lateral accelerations. For each group there are peak-to-peak values (maximum minus minimum values) and averages values along the 100m track. The soft joint considers the $K_T$ and $C_T$ defined on section 4.2 and 4.3. The hard joint considers a very high value of $K_T$, been equivalent to weld the tower on the trailer.

In table 3, with the non linear model, the hard joint produces lateral displacements over two times higher than the soft joint. The hard/soft ratio of max-min displacements at speeds of 3, 6 and 12 km/h are respectively 1,0 1,9 and 2,2. The hard/soft ratios of average displacements are the same. The lateral accelerations produced by a hard joint are over five times higher than the soft joint. The hard/soft ratio of max-min accelerations at speeds of 3, 6 and 12 km/h are respectively 1,0 5,2 and 4,4. The hard/soft ratio of average accelerations at speeds of 3, 6 and 12 km/h are respectively 1,0 6,3 and 5,2. Tables 4, with the linear model, the responses are similar.

These results show us that an adequate suspension on joint P could isolate significantly the energy transmission from trailer to the tower in the agricultural field and reduce displacements and acceleration on tower. Note that force and fatigue are directly proportional accelerations. Lower levels of accelerations contribute for a long-life of the equipment.

## 5. CONCLUSION

Both mathematical models respond consistently to the input signals. Mainly the linear model indicates smaller responses than the non linear model. For the final validation of these model it is necessary compare their results with measures of the real equipments, which is planed for future papers.

The models can aid in engineer solutions visualization and in the project parameters selection. The inverted pendulum construction has great potential to increase stability, to reduce oscillation amplitudes, to reduce accelerations and to reduce forces into the system.

## 6. ACKNOWLEDGEMENTS

Gratefulness to Máquinas Agrícolas Jacto S/A for the dada supplied.

## 7. REFERENCES

Bogdanov, A., “Optimal Control of a Double Inverted Pendulum on a Cart” Department of Computer Science & Electrical Engineering, OGI School of Science & Engineering, OHSU - Technical Report CSE-04-006, Dec/2004.

Chaplin, J., Wu, C., “Dynamic Modeling of Field Sprayer” - American Society of Agricultural Engineers, Vol. 36(6), p. 1857-1863, November-December 1989.

D’Souza, A. F.; Garg, V.K.,“Advanced Dynamics - Modeling and Analysis” Prentice-Hall, Inc., 1984.

Frost, A. R., “A design Procedure for Twin Universal Link Spray Boom Suspensions” - The British Society for Research in Agricultural Engineering, Vol. 37, p. 179-189, 1987.

International Standard ISO 5008, “Agricultural wheeled tractors and field machinery - Measurement of whole-body vibration of the operator”, First edition, 15/05/1979

Ogata, K., “Modern Control Enginnering - Third Edition” Prentice Hall., 1997. p. 152.

Meirovitch, L. , “Methods of Analytical Dynamics” McGraw-Hill, 1970, p. 45-97 .

## 8. RESPONSIBILITY NOTICE

The authors are the only responsible for the printed material included in this paper.